Environmental Pollution 246 (2019) 11–18

Contents lists available at ScienceDirect

Environmental Pollution

journal homepage: www.elsevier.com/locate/envpol

Particulate matter pollution in Chinese cities: Areal-temporal variations and their relationships with meteorological conditions (2015–2017)☆

Xiaoyang Li [a, 1], Hongquan Song [a, b, c, *, 1], Shiyan Zhai [a, b], Siqi Lu [d], Yunfeng Kong [a, b], Haoming Xia [a], Haipeng Zhao [a, b]

[a] Laboratory of Geospatial Technology for the Middle and Lower Yellow River Regions, Ministry of Education, Henan University, Kaifeng, Henan, 475004, China
[b] Institute of Urban Big Data, College of Environment and Planning, Henan University, Kaifeng, Henan, 475004, China
[c] Henan Key Laboratory of Integrated Air Pollution Control and Ecological Security, Henan University, Kaifeng, Henan, 475004, China
[d] College of Plant Science, Jilin University, Changchun, Jilin, 130062, China

ARTICLE INFO

Article history:
Received 23 August 2018
Received in revised form
14 November 2018
Accepted 29 November 2018
Available online 1 December 2018

Keywords:
$PM_{2.5}$
PM_{10}
$PM_{2.5}$ to PM_{10} ratio
Meteorological factors
China

ABSTRACT

As the second largest economy in the world, China experiences severe particulate matter (PM) pollution in many of its cities. Meteorological factors are critical in determining both areal and temporal variations in PM pollution levels; understanding these factors and their interactions is critical for accurate forecasting, comprehensive analysis, and effective reduction of this pollution. This study analyzed areal and temporal variations in concentrations of $PM_{2.5}$, PM_{10}, and PM_{coarse} (PM_{10} - $PM_{2.5}$) and $PM_{2.5}$ to PM_{10} ratios ($PM_{2.5}/PM_{10}$) and their relationships with meteorological conditions in 366 Chinese cities from January 1, 2015 to December 31, 2017. On the national scale, $PM_{2.5}$ and PM_{10} decreased from 48 to 42 μg m^{-3} and from 88 to 84 μg m^{-3}, respectively, and the annual mean concentrations were 45 μg m^{-3} ($PM_{2.5}$) and 84 μg m^{-3} (PM_{10}) during the time period (2015–2017). In most regions, largest PM concentrations occurred in winter. However, in northern China, in spring PM_{coarse} concentrations were highest due to dust. The $PM_{2.5}/PM_{10}$ ratio was higher in southern than in northern China. There were large regional disparities in PM diurnal variations. Generally, PM concentrations were negatively correlated with precipitation, relative humidity, air temperature, and wind speed, but were positively correlated with surface pressure. The sunshine duration showed negative and positive impacts on PM in northern and southern cities, respectively. Meteorological factors impacted particulates of different size differently in different regions and over different periods of time.

1. Introduction

Rapid economic development and urbanization have led to severe urban air pollution in China, especially particulate matter (PM) pollution (He et al., 2017; Lu et al., 2017). In many Chinese cities, PM concentrations greatly exceed standards recommended by the World Health Organization (WHO) (Zhang et al., 2015a). High concentrations of $PM_{2.5}$ (particulate matter with an aerodynamic diameter ≤ 2.5 μm) and PM_{10} (particulate matter with an aerodynamic diameter ≤ 10 μm) have important impacts on human health, climate change, and ecosystems (Tie et al., 2009; Yang et al., 2017b; Kok et al., 2018). Such high concentrations threaten the sustainable development of China's economy and the wellbeing of society.

Anthropogenic emissions and meteorological forces interact to create and determine levels of air pollution (Fast et al., 2007). Meteorological conditions play dominant roles in dispersion, transformation, and removal of air pollutants in the atmosphere (Ocak and Turalioglu, 2008; Xu et al., 2015). It is essential to understand spatial and temporal variations of PM and their relations to meteorological conditions if we are to control and reduce

☆ This paper has been recommended for acceptance by Eddy Y. Zeng.

* Corresponding author. College of Environment and Planning, Henan University Jinming Campus, Kaifeng, Henan Province, 475004, China.
E-mail address: hqsong@henu.edu.cn (H. Song).

[1] These authors contributed equally to this work and should be considered co-first authors.

https://doi.org/10.1016/j.envpol.2018.11.103
0269-7491/

pollution with effective measures. Numerous studies have reported characteristics of PM pollution and its relationship with meteorological factors in China over the past decade (Huang et al., 2015; Xu et al., 2015; Zhang et al., 2015b; Chen et al., 2016; Li et al., 2017; Zhang et al., 2018), but these are limited to provincial capitals or mega cities, such as Beijing, Shanghai, Nanjing, Wuhan, and Guangzhou.

In 2013, the hourly mean concentrations of $PM_{2.5}$, PM_{10}, and four other air pollutants measured by air quality monitoring (AQM) stations in major Chinese cities were released to the public. This report provided adequate information to evaluate nationwide spatial and temporal patterns of air quality and its driving factors in China. Several studies have attempted to identify spatial and temporal patterns of PM (Wang et al., 2014; Wang et al., 2015; Xie et al., 2015; Zhang and Cao, 2015; Zhao et al., 2016; Ye et al., 2018) and their correlations with meteorological factors (He et al., 2017; Yang et al., 2017a; Ye et al., 2018) at a nationwide scale. Although these studies systematically investigated spatial and temporal variations of PM, most of them were mainly focused on $PM_{2.5}$. Issues of extreme PM_{10} concentration events have been continuously raised for the last few years in China. Coarse particles (PM_{10}-$PM_{2.5}$, PM_{coarse}) and $PM_{2.5}$ are generally produced by different sources, so the $PM_{2.5}/PM_{10}$ ratio reveals characteristics of particulate pollution. However, spatial and temporal patterns $PM_{2.5}$, PM_{10}, PM_{coarse}, and $PM_{2.5}/PM_{10}$ ratios and their correlations with multi-scale meteorological conditions on nationwide scale remain unclear.

The objective of this study was to assess nationwide areal and temporal variations of different-sized PM and $PM_{2.5}/PM_{10}$ ratios, as well as their relationships with meteorological conditions in China. The hourly average PM concentrations in 366 cities in China and diurnal average meteorological variables at 839 national meteorological stations in the calendar years of 2015 through 2017 were used in this study.

2. Materials and methods

2.1. Study area

We studied 366 cities in China and did not include Taiwan, Hongkong, or Macao due to the lack of data. We divided China into 10 regions according to economic development, climate, and topography (Liu; 2005) (Fig. S1). These 10 regions are: Northeastern District (NE), Northern Coastal District (NC), Eastern Coastal District (EC), Southeastern Coastal District (SC), the Middle Reaches of the Yellow River District (MYR), the Middle and Upper Reaches of the Yangtze River District (MUYR), the Middle and Upper Reaches of the Pearl River District (MUPR), the Upper Reaches of the Yellow River District (UYR), Xinjiang District (XJ), and Qinghai-Tibetan Plateau District (QTP). Regions of SC, MUPR, MUYR, and EC and of MYR, NC, UYR, and NE were considered as southern and northern China, respectively.

2.2. Datasets

Daily and hourly mass concentrations of $PM_{2.5}$ and PM_{10} in 366 cities in China (Fig. S2a) obtained from the China National Environmental Monitoring Center (http://106.37.208.233:20035/) during 2015–2017 were analyzed in this study. According to the Chinese Ambient Air Quality Standard (CAAQS) (GB3095-2012) (Lai et al., 2016), the annual means of $PM_{2.5}$ concentration limits are 15 $\mu g\,m^{-3}$ for Grade I and 35 $\mu g\,m^{-3}$ for Grade II, while the related daily means are 35 $\mu g\,m^{-3}$ for Grade I and 75 $\mu g\,m^{-3}$ for Grade II. The annual means of PM_{10} concentrations limits are 40 $\mu g\,m^{-3}$ for Grade I and 70 $\mu g\,m^{-3}$ for Grade II, while the related daily means are 50 $\mu g\,m^{-3}$ for Grade I and 150 $\mu g\,m^{-3}$ for Grade II. Air quality in all cities was assessed according to Grade II limits.

Daily average meteorological data, including accumulated precipitation (PRE, mm), surface pressure (PRS, hPa), 2-m relative humidity (RHU, %), sunshine duration (SSD, h), 2-m air temperature (TEM, °C), and 10-m wind speed (WIN, m s^{-1}) at 839 stations (Fig. S2b) from January 2015 through December 2017 were adopted to explore relationships between PM and meteorological conditions. This data were obtained from the China Meteorological Data Network (http://data.cma.cn).

2.3. Methodology

As shown in Fig. S2, there are discrepancies between air quality monitoring and meteorological site data. It was essential to match the two types of data for the analysis of relationships between PM and meteorological conditions. We used the kriging method to interpolate surfaces of meteorological parameters based on meteorological observations using ArcGIS 10.3 software developed by Esri (http://www.esri.com). Then meteorological factors at 366 cities were extracted from the kriged surfaces at the locations corresponding to the PM measurements. Cross validation was conducted to evaluate the performance of the kriging method. For statistical measures, we used the mean bias (MB), the normalized mean bias (NMB), the normalized mean error (NME), the root mean square error (RMSE), and correlation coefficient (R) (Song et al., 2017). Table S1 shows the performance of kriged meteorological parameters, indicating that the kriging method is able to reproduce meteorological surfaces in China.

To comprehensively investigate areal-temporal variations of different-sized PM and their relationships with meteorological conditions, we conducted analyses at multiple spatial scales of city, region, and nation, and temporal scales of day, month, season, and year. This study divided the whole year into four seasons, namely spring (March, April, and May, MAM), summer (June, July, and August, JJA), autumn (September, October, and November, SON), and winter (December, January, and February, DJF). Spearman's correlation coefficient (Rebekić et al., 2015) was adopted to measure the relationships between PM and meteorological conditions.

3. Results

3.1. Areal-temporal variations of PM

3.1.1. Areal variations of PM

The spatial distribution of exceedance percentage of PM_{10} limits, that is the annual percentage of days that exceeded the daily average PM_{10} limit (150 $\mu g\ m^{-3}$) in CAAQS, indicated that severe PM_{10} pollution (>20%) mainly occurred in NC, MYR, XJ, and western UYR (Figs. 1a and S3). In southern China, however, the exceedance of PM_{10} limit was <10%. Exceedance of $PM_{2.5}$ limits (75 $\mu g\,m^{-3}$) suggested that severe $PM_{2.5}$ pollution was mainly distributed in NC, MYR, XJ, and MUYR (Figs. 1b and S4). The $PM_{2.5}/PM_{10}$ was found to be higher in southern than in northern China (Fig. 1c).

There were large seasonal variations in spatial patterns of PM (Figs. S4 and S5). The highest levels of PM_{10} and $PM_{2.5}$ occurred in winter, followed by spring and autumn in all regions. The $PM_{2.5}/PM_{10}$ was generally higher in southern than in northern China through the whole year (Fig. S4). Except for NE, PM_{coarse} concentrations were greater in northern than in southern areas during four seasons (Fig. S5). Compared with PM_{10} and $PM_{2.5}$, the highest PM_{coarse} concentration occurred in spring followed by winter, autumn, and summer, and these high concentrations were mainly distributed in NC, MYR, UYR, and XJ.

3.1.2. Temporal trends in PM

The highest annual mean concentrations of PM_{10} and $PM_{2.5}$ were in XJ (136 μg m^{-3}) and MYR (63 μg m^{-3}), while the lowest were in SC (49 μg m^{-3}) and QTP (29 μg m^{-3}) (Fig. 2, Table S2). The annual mean $PM_{2.5}$ concentrations were higher than CAAQS limits in most regions except for SC, QTP, and MUPR (Fig. 2, Table S2). Except for SC and XJ, $PM_{2.5}$ concentrations declined in all the other regions (Fig. 2) from 2015 to 2017. The $PM_{2.5}/PM_{10}$ also showed decreasing trends in most regions.

Different-sized PM showed different patterns of variation over days and months in all 10 regions (Fig. 3). Both PM_{10} and $PM_{2.5}$ were at lowest levels in all 10 regions during summer months, and in SC, MUPR, and QTP through the whole year. In XJ, PM_{10} concentrations were at a high level from January to May and peaked in March. The PM_{10} was high in UYR, MYR, NE, and NC in spring and winter. The $PM_{2.5}/PM_{10}$ was >0.5 in MUYR, SC, EC, and MUPR through the whole year. In most regions, PM_{10} had two peaks and two troughs at 11:00–13:00 and midnight and 6:00–7:00 and 18:00–19:00, respectively. In UYR, MYR, NE, NC, and QTP, two peaks and two troughs of $PM_{2.5}$ were also found at 0:00–1:00 and 13:00–14:00 and 7:00–8:00 and 20:00, respectively. In XJ, however, there were three peaks and three troughs in $PM_{2.5}$ at 0:00, 11:00, and 16:00 and 10:00, 12:00, and 22:00, respectively. The $PM_{2.5}/PM_{10}$ peaked at 11:00 and 20:00–21:00 in all the 10 regions and minimized at 8:00 in most regions.

3.2. Correlations between PM and meteorological conditions

3.2.1. Annual correlations between PM and meteorological factors

Figs. S6–S12 show spatial patterns of annual and seasonal PRE, PRS, RHU, SSD, TEM, and WIN in China during 2015–2017. Upward and downward histograms indicate positive and negative correlation coefficients, respectively (Figs. 3 and 4). Both PM_{10} and $PM_{2.5}$ showed significantly ($P < 0.01$) negative and positive relationships with PRE and PRS in most regions (Fig. 4, Table S3), respectively. PM_{10} was negatively correlated with RHU in all regions except for XJ (Fig. 4a). RHU had significantly ($P < 0.01$) negative impacts on $PM_{2.5}$ in QTP, MUYR, MUPR, SC, MYR, and NE, but showed positive impacts on $PM_{2.5}$ in XJ (Fig. 4b, Table S3). SSD had positive or negative impacts on PM_{10} and $PM_{2.5}$. Both PM_{10} and $PM_{2.5}$ showed significantly ($P < 0.01$) negative correlations with TEM in all regions (Fig. 4, Table S3). Correlations between PM_{10} and WIN were significantly ($P < 0.01$) positive in QTP and UYR and negative in EC, MUYR, SC, and XJ. However, $PM_{2.5}$ showed negative dependence on WIN in most regions except for QTP and MUPR. Figs. S13 and S14 show spatial patterns of correlations between PM and meteorological parameters and their *P*-value for individual cities.

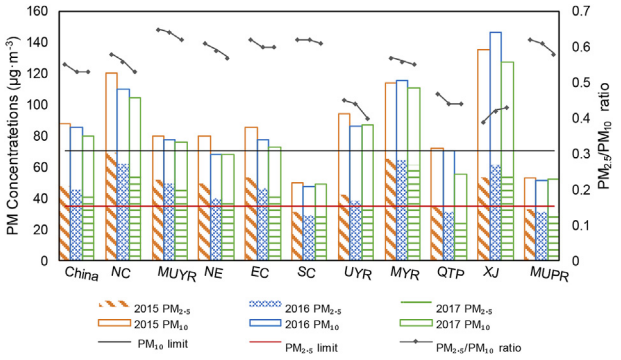

Fig. 2. Interannual variations of concentrations of $PM_{2.5}$ and PM_{10} (histograms – primary y-axis) and $PM_{2.5}/PM_{10}$ ratio (solid lines with dots – secondary y-axis) in 10 regions of China.

All meteorological parameters showed weak or not significant impacts on $PM_{2.5}/PM_{10}$ in QTP (Fig. 4c, Table S3). Precipitation apparently reduced $PM_{2.5}/PM_{10}$ in MUPR, MUYR, SC, NE, UYR, and XJ (Fig. 4c, Table S3). The $PM_{2.5}/PM_{10}$ was positively correlated with PRS, but negatively correlated with TEM in all regions except QTP. RHU could stimulate $PM_{2.5}/PM_{10}$ significantly ($P < 0.01$) in most regions except MUPR ($R = -0.15$, $P < 0.01$) and SC ($R = -0.05$, $P = 0.11$). However, the $PM_{2.5}/PM_{10}$ showed significantly ($P < 0.01$) negative dependences on SSD in all 10 regions. In MUPR and SC, there were no significant impacts of WIN on $PM_{2.5}/PM_{10}$, but there were significantly ($P < 0.01$) negative relationships in other regions.

3.2.2. Seasonal correlations between PM and meteorological factors

Precipitation can reduce both PM_{10} and $PM_{2.5}$ in most regions through the whole year (Fig. 5, Tables S4 and S5). Negative impacts of PRE on PM_{10} were relatively stronger than on $PM_{2.5}$. The $PM_{2.5}/PM_{10}$ was positively correlated with PRE in EC and MYR during four seasons, but showed large temporal variations in its dependence on PRE in other regions (Fig. 5, Table S6). PM_{10} showed negative dependence on RHU in most regions except XJ, UYR, and NC and some regions in winter (Fig. 5, Table S4). However, $PM_{2.5}$ was negatively and positively correlated with RHU in QTP, SC, MUPR, and MUYR and in NC, MYR, and UYR, respectively. Both PM_{10} and $PM_{2.5}$ showed significantly positive correlations with RHU in NE, NC, and MYR in winter. The $PM_{2.5}/PM_{10}$ was positively correlated with RHU in most regions through the whole year.

PM_{10} and $PM_{2.5}$ generally showed negative and positive correlations with SSD in northern and southern China, respectively, in spring, autumn, and winter (Fig. 5, Tables S4 and S5). In summer, however, PM_{10} was positively correlated with SSD in most regions.

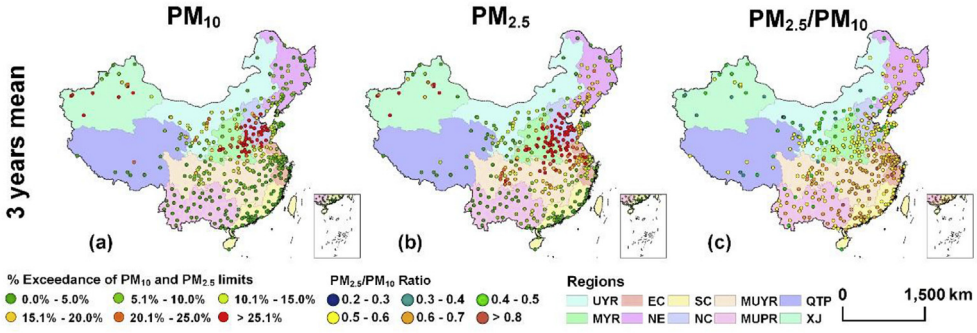

Fig. 1. Spatial distributions of cities where the annual mean of daily levels exceeded CAASQ limits for PM_{10} (a) and $PM_{2.5}$ (b) and $PM_{2.5}/PM_{10}$ (c) in major Chinese cities during 2015–2017.

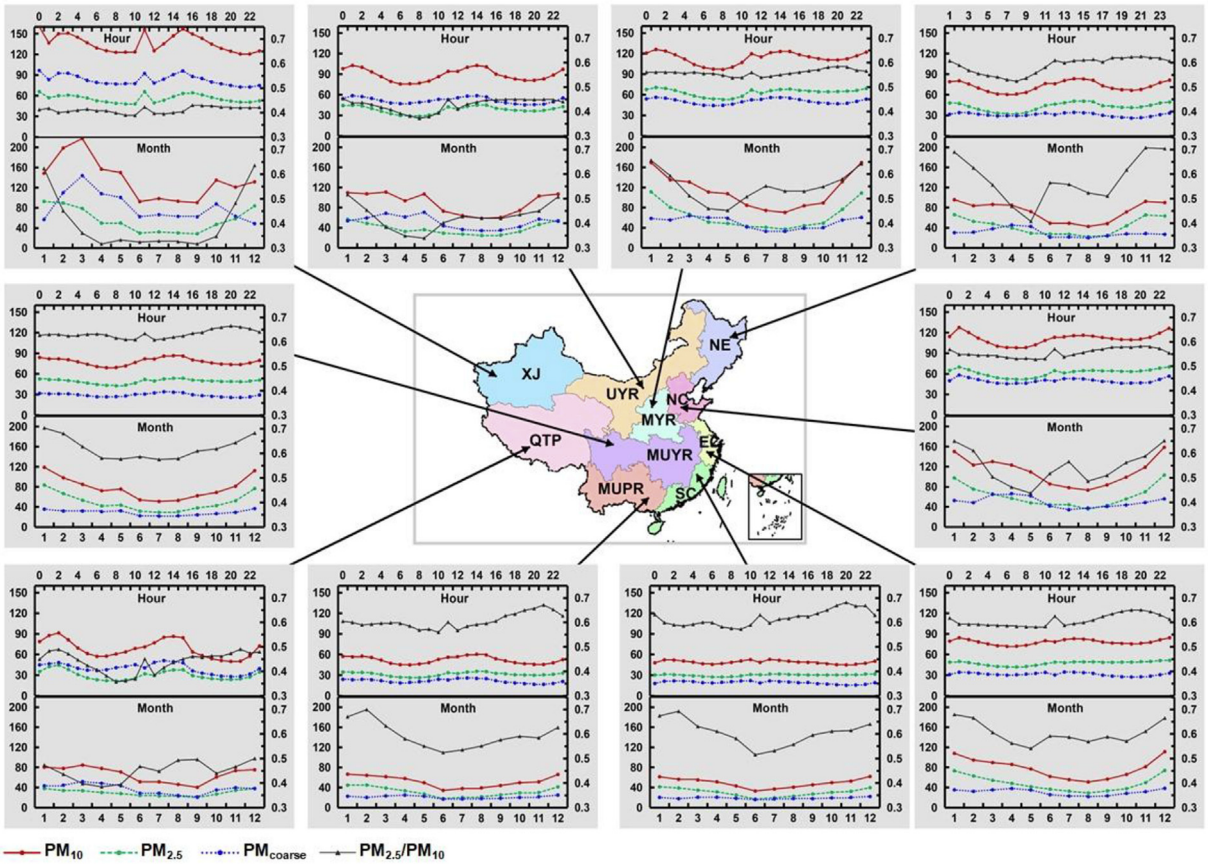

Fig. 3. Inter-month and diurnal variations of concentrations of PM_{10} (solid line with circle – primary y-axis; μg m^{-3}), $PM_{2.5}$ (dashed line with circle – primary y-axis; μg m^{-3}), PM_{coarse} (dotted line with circle – primary y-axis; μg m^{-3}), and the ratio of $PM_{2.5}$ to PM_{10} (solid line with triangle – secondary y-axis) in 10 regions.

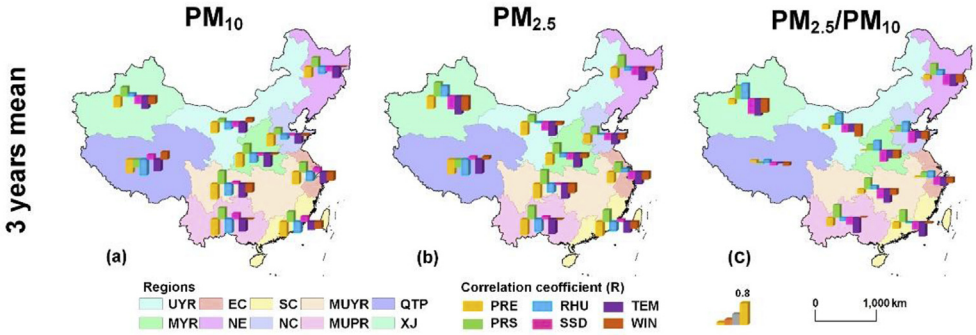

Fig. 4. Histograms of correlations between annual PM_{10} (a), $PM_{2.5}$ (b), and $PM_{2.5}/PM_{10}$ (c) and meteorological parameters (PRE, PRS, RHU, SSD, TEM, and WIN) in 10 regions.

$PM_{2.5}$ showed positive correlations with SSD in XJ, MUPR, QTP, and SC. $PM_{2.5}/PM_{10}$ showed negative dependence on SSD in most regions during four consecutive seasons. PM_{10} was negatively correlated with TEM in MUPR, QTP, SC and XJ in spring, but showed positive correlations in most regions except EC, MUYR, and MYR in summer (Fig. 4, Table S3). Except for SC in autumn and XJ in winter, PM_{10} showed negative and positive dependence on TEM in all the other regions in autumn and winter, respectively. $PM_{2.5}$ was negatively correlated with TEM in most regions except EC and MUYR in spring and in all regions in autumn. However, $PM_{2.5}$ had positive correlations with TEM in NC, NE, SC, UYR, and XJ in summer and in most regions in winter. TEM had negative impacts on $PM_{2.5}/PM_{10}$ in almost all the regions throughout the whole year.

Both PM_{10} and $PM_{2.5}$ were positively correlated with PRS in SC, MUPR, and XJ in spring and in NE, XJ, SC, EC, MUPR, and MUYR in autumn (Fig. 5, Tables S4 and S5). However, both PM_{10} and $PM_{2.5}$ showed negative dependence upon PRS in UYR and SC in summer and in NC, UYR, MYR, QTP, and EC in winter. Relationships between $PM_{2.5}/PM_{10}$ and PRS were significantly ($P < 0.01$) positive in spring and autumn in MUYR, NE, XJ and UYP, but were significantly ($P < 0.01$) negative in SC and NE. In EC, MUPR, MUYR, and SC, PM_{10} was negatively correlated with WIN through the whole year except MUPR in spring (Fig. 5, Table S4). Moreover, the negative correlations between PM_{10} and WIN also occurred in MYR and NC in autumn and winter and in XJ in spring and autumn. However, the correlation was significantly ($P < 0.01$) positive in QTP during the

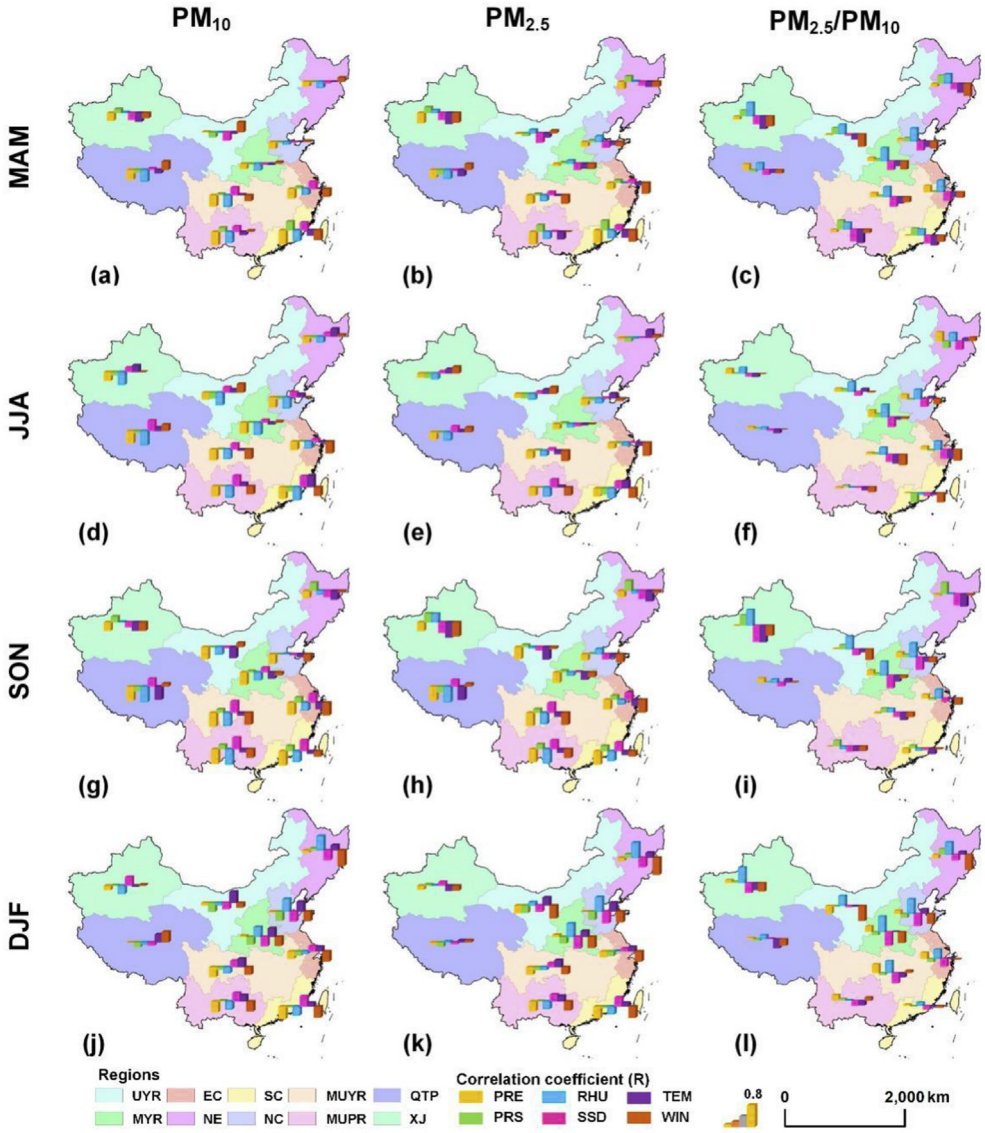

Fig. 5. Seasonal variations of correlations between PM_{10}, $PM_{2.5}$, and $PM_{2.5}/PM_{10}$ and meteorological factors (PRE, PRS, RHU, SSD, TEM, and WIN) in spring (a, b, and c), summer (d, e, and f), autumn (g, h, and i), and winter (j, k, and l) at regional scale in 10 regions.

whole year and in UYR in spring, summer, and autumn. $PM_{2.5}$ showed negative correlations with WIN in most regions of China except QTP and UYR. In most regions, $PM_{2.5}/PM_{10}$ had negative dependence upon WIN. Figs. S15–S26 show spatial and seasonal variations of correlations and *P*-values between PM and meteorological conditions at individual cites.

4. Discussion

Levels of PMs steadily decreased in most regions from 2015 to 2017, which is consistent with the environmental policy and regulation changes in China. This indicates that the environmental protection policies and haze control measures, such as the Ten Measures for Air Pollution Prevention and Control implemented by the State Council of China in 2013, are taking effect. The highest PM_{coarse} concentrations were observed in spring in northern regions. Dust events frequently occur in northwestern China such as the Taklimakan Desert in XJ and the Gobi Desert in southern Mongolia and western UYR, especially in late winter and early spring when surface conditions are dry and winds are strong (Yasunori and Masao, 2005; Di et al., 2016; Song et al., 2016, 2017). Large amounts of dust particles are emitted into the atmosphere from arid and semiarid regions during dust events and frequently transported over long distances (Yang et al., 2007), which could lead to the high levels in PM_{10} and PM_{coarse} in UYR, XJ, NC, and MYR. Thus, the source of these high levels may be natural, not anthropogenic.

Higher $PM_{2.5}$ concentrations were observed in NC, MYR, northern EC, and MUYR, especially in winter, which is consistent with previous studies (Huang et al., 2015; Ma et al., 2016). Numerous studies have ascribed the higher $PM_{2.5}$ concentrations in these regions to greater emissions from coal-burning industries (such as coal-fired power plants, steel and iron manufacturing, etc), fossil fuel combustion, and coal and biomass burning for residential heating in winter (typically from mid-November through mid-March) (Cao et al., 2011; Chai et al., 2014; Wang et al., 2014). Moreover, temperature inversion and stable weather often occur in winter (Li et al., 2012), which is unfavorable for the rapid diffusion

of $PM_{2.5}$. In northern China in summer and in SC, MUPR, and QTP through the whole year, however, low level $PM_{2.5}$ concentrations could result from the adsorption of fine particles and suppression of dust emissions by growing vegetation (Yi et al., 2017), more favorable diffusion and scavenging conditions, and lower emissions due to no residential heating.

The $PM_{2.5}/PM_{10}$ was >0.5 in MUYR, EC, SC, and MUPR through the whole year, but was <0.5 in XJ, UYR, and QTP during all seasons except winter. The $PM_{2.5}/PM_{10}$ in the south was higher than in the north because, in the south, fine particles accounted for a larger proportion of the particulates. The decrease in the $PM_{2.5}/PM_{10}$ in most regions may be due to the stricter air pollution emission control measures adopted in China in recent years, such as coal to gas heating in NC, NE, and MYR, motor vehicle restrictions in many cities, more stringent controls on construction emissions, etc. Lower $PM_{2.5}/PM_{10}$ in spring suggests that PM_{coarse} is high in spring, which is probably caused (as mentioned earlier) by natural dust and its long-range transport, especially in northwestern China.

A bimodal and dual valley pattern in diurnal PM_{10} concentrations with peaks at 11:00–13:00 and midnight and troughs at 6:00–7:00 and 18:00–19:00 were observed in most regions. Similar patterns were also found in diurnal variations of $PM_{2.5}$ concentrations in most regions, but the hourly changes in $PM_{2.5}$ concentrations were not obvious in EC, SC, and MUPR. In the early morning hours, human activities are low. At this time (0:00–6:00), the planetary boundary layer (PBL) is also usually low and often stratified due to the temperature inversion. PMs, particularly coarser PMs, settle under the force of gravity and concentrations decrease, creating the first trough at around 7:00. Increasing solar radiation with sunrise leads to the formation of a convectively mixed boundary layer (CBL) (Pitz et al., 2008), which is associated with increasing ambient temperature, global radiation, and wind speed. This results in an increase in secondary particle production (sulfate, nitrate, and organic carbon). In addition, a large amount of PM is emitted into the atmosphere with increased traffic flow as human activity increases. It is difficult for these PMs to settle in a short time. The amount of PM emitted is greater than the amount that is reduced by the diffusion of the atmosphere, hence concentrations reach the first peak around noon. The PM_{10} and $PM_{2.5}$ peaks at 11:00 in XJ could be related to the morning traffic, because China uses one time zone throughout the country and the morning hours in XJ are two to three hours later than in eastern regions of China. In the afternoon, the PBL is high due to the high temperatures, which can lead to strong dilution and diffusion of PM. The PM concentration begins to decrease toward the evening, reaching the second trough of the day around 18:00. Then the PBL height gradually decreases as the temperature falls, resulting in declining dilution and diffusion. After sunset, truck traffic increases, putting more dust and primary PM emissions into the atmosphere and causing a peak at midnight.

Local meteorological conditions significantly affect the diffusion, dilution, and accumulation of PM in cities. These urban heat islands are the source of the pollution from which they suffer (Tian et al., 2014; Fortelli et al., 2016). We observed large areal and seasonal variations in correlations between PM and meteorological conditions across China. Precipitation was negatively correlated with $PM_{2.5}$ and PM_{10} concentrations, which is consistent with numerous previous studies (Tai et al., 2010; Lin et al., 2015; Li et al., 2017). This is due to the fact that PRE has scavenging effects on PM by wet deposition. In addition, PRE usually makes natural and fugitive dust more difficult to release from the ground surface into the atmosphere, because the minimum friction wind velocity required for dust emissions increases under wet conditions. However, the positive correlation between $PM_{2.5}/PM_{10}$ and PRE in most regions indicates that PRE reduces PM_{10} concentrations to a greater extent than $PM_{2.5}$ concentrations. Correlations between PM and RHU show large regional differences and vary with seasons, which is consistent with some previous studies (Ch et al., 2005; Trivedi et al., 2014; Li et al., 2017). Negative relationships between PM and RHU were observed in most regions during the whole year, and are likely due to the suppression of natural and fugitive dust emissions under moist air conditions. However, the positive relationship between $PM_{2.5}$ and RHU in winter can be attributed to the facts that RHU favors the partitioning of semi-volatile species into aerosols (Cao et al., 2012) and that the moist atmosphere is normally accompanied by low PBL (Sandeep et al., 2014).

Few studies have explored relationships between PM and PRS, as well as PM and SSD. PRS exhibited positive correlations with $PM_{2.5}$, PM_{10}, and $PM_{2.5}/PM_{10}$ except in QTP through the year, which is consistent with several previous studies (Huang et al., 2015; Li et al., 2017). In most cases, high PRS is accompanied by low PBL height, which prevents the scavenging of air pollutants (Wu et al., 2017), leading to the accumulation of PM in the boundary layer. Significantly negative correlations between PM and PRS were observed in MYR, NC, and UYR in winter. In these regions, PM concentrations were high due to residential heating in winter. Second, there is generally little wind in these areas, and, low PRS is often accompanied by low local wind speeds in winter; both of these factors will tend to the rapid accumulation of PM. In general, negative and positive correlations between PM and SSD were observed in northern and southern China, respectively. The negative relationships may be attributed to the large atmospheric volume for PM dilution resulting from a very high PBL in northern China (Huang et al., 2015). The positive relationships in southern China occurred most likely because the SSD accelerates the formation of secondary particles by photochemical reaction (Whiteman et al., 2014), especially in regions with a higher temperature (Xu et al., 2015).

Temperature is closely related to PM by affecting atmospheric turbulence and chemical reactions (He et al., 2017). This study observed that the PM was negatively correlated with TEM in spring and autumn in most regions, and positively correlated in summer and winter. Secondary particles are generated by photochemical processes under high TEM conditions (Feng et al., 2012; Zhu et al., 2014) in summer and winter. However, the decreased temperature inversion by increased temperature enhances the diffusion and dispersion of PM in spring and autumn (Yang et al., 2015). Relationships between PM and WIN were significantly negative in most regions, indicating that WIN plays an important role in the PM horizontal dispersion of PM. However, positive correlations between PM and WIN in QTP and UYR most likely result from dust events due to the dry surface conditions and strong winds, especially in late winter and early spring. This would affect other regions by transport of coarse dust particles.

5. Conclusions

This study is the most comprehensive analysis, to the best of our knowledge, in spatial-temporal patterns of PM and its relation to meteorological conditions in China. The results indicate that PM concentrations have large areal and temporal variations. The annual average mass concentrations of $PM_{2.5}$ and PM_{10} in China from 2015 to 2017 were 45 $\mu g\ m^{-3}$ and 84 $\mu g\ m^{-3}$, respectively. All annual mean concentrations of $PM_{2.5}$, PM_{10}, and PM_{coarse} and $PM_{2.5}/PM_{10}$ decreased at the national scale from 2015 to 2017. Both $PM_{2.5}$ and PM_{10} were observed largest in winter, followed by spring, autumn, and summer. However, the PM_{coarse} was largest in spring, followed by winter, autumn, and summer. The $PM_{2.5}/PM_{10}$ was higher in southern than in northern China. PM concentrations in central regions of China were generally higher than in other

regions. PM_{coarse} concentrations were highest in northern China in spring, because of the emission of coarse particles into the atmosphere from bare and loose surface soils and transport by strong winds. Large regional differences were observed in diurnal variations of PM. The diurnal variations of PM_{10} were characterized by two peaks and two troughs in most regions.

The findings indicate that local meteorological conditions play an important role in PM pollution in cities. PM concentrations show clear negative relationships with PRE throughout the year and with RHU in spring, summer, and autumn in most regions; this is likely the result of scavenging effects and the suppression of dust emissions due to moist conditions of air and ground surface. The negative correlations between PM concentrations and WIN are mainly due to strong horizontal dispersion by strong winds. This is not true for PM_{10} as strong winds result in release of coarse dust particles from the ground surface and transport into the atmosphere. The relationship between PM and PRS was positive in most regions, but was negative in MYR, NC, and UYR in winter. In most regions, the PM was negatively correlated with TEM in spring and autumn, but positively correlated with TEM in summer and winter. Negative and positive relationships between PM and SSD were observed in northern and southern China, respectively. The negative relationship was mainly due to the increased height of the PBL caused by the increased TEM, but the positive relationship was mainly because longer SSD accelerates photochemical reactions. This study offers information that can be used to determine the efficacy of measures being taken to curtail pollution, to inform the creation of new policies to further reduce pollution, and to estimate the potential human exposure to PM.

Acknowledgements

This study was financially supported by the National Natural Science Foundation of China (41401107) and the Research Program of Henan University, China (2015YBZH001). We the authors thank Shenghui Zhou from Henan University for helpful discussions on data analysis.

Appendix A. Supplementary data

Supplementary data to this article can be found online at https://doi.org/10.1016/j.envpol.2018.11.103.

References

Cao, G.L., Zhang, X.Y., Gong, S.L., An, X.Q., Wang, Y.Q., 2011. Emission inventories of primary particles and pollutant gases for China. Sci. Bull. 56 (8), 781–788. https://doi.org/10.1007/s11434-011-4373-7.

Cao, J.J., Shen, Z.X., Chow, J.C., Watson, J.G., Lee, S.C., Tie, X.X., Ho, K.F., Wang, G.H., Han, Y.M., 2012. Winter and summer $PM_{2.5}$ chemical compositions in fourteen Chinese cities. J. Air Waste Manag. Assoc. 62 (10), 1214–1226. https://doi.org/10.1080/10962247.2012.701193.

Ch, V., Saraga, D., Maggos, T., Michopoulos, J., Pateraki, S., Helmis, C.G., 2005. Temporal variations of $PM_{2.5}$ in the ambient air of a suburban site in Athens, Greece. Sci. Total Environ. 349 (1–3), 223–231. https://doi.org/10.1016/j.scitotenv.2005.01.012.

Chai, F., Gao, J., Chen, Z., Wang, S., Zhang, Y., Zhang, J., Zhang, H., Yun, Y., Ren, C., 2014. Spatial and temporal variation of particulate matter and gaseous pollutants in 26 cities in China. J. Environ. Sci. 26 (1), 75–82. https://doi.org/10.1016/S1001-0742(13)60383-6.

Chen, T., He, J., Lu, X., She, J., Guan, Z., 2016. Spatial and temporal variations of $PM_{2.5}$ and its relation to meteorological factors in the urban area of Nanjing, China. Int. J. Environ. Res. Publ. Health 13 (9). https://doi.org/10.3390/ijerph13090921.

Di, A., Xue, Y., Yang, X., Leys, J., Guang, J., Mei, L., Wang, J., She, L., Hu, Y., He, X., Che, Y., Fan, C., 2016. Dust aerosol optical depth retrieval and dust storm detection for Xinjiang region using Indian national satellite observations. Rem. Sens. 8 (9), 702. https://doi.org/10.3390/rs8090702.

Fast, D.J., Foy De, B., Acevedo Rosas, F., Caetano, E., Carmichael, G., Emmons, L., Mckenna, D., Mena, M., Skamarock, W., Tie, X., Coulter, R.L., Barnard, J.C., Wiedinmyer, C., Madronich, S., 2007. A meteorological overview of the MILAGRO field campaigns. Atmos. Chem. Phys. 7 (9), 2233–2257. https://doi.org/10.5194/acp-7-2233-2007.

Feng, J.L., Guo, Z.G., Zhang, T.R., Yao, X.H., Chan, X.H., Fang, M., 2012. Source and formation of secondary particulate matter in $PM_{2.5}$ in Asian continental outflow. J. Geophys. Res. Atmos. 117, D03302. https://doi.org/10.1029/2011JD016400.

Fortelli, A., Scafetta, N., Mazzarella, A., 2016. Influence of synoptic and local atmospheric patterns on PM_{10} air pollution levels: a model application to Naples (Italy). Atmos. Environ. 143, 218–228. https://dx.doi.org/10.1016/j.atmosenv.2016.08.050.

He, J., Gong, S., Yu, Y., Yu, L., Wu, L., Mao, H., Song, C., Zhao, S., Liu, H., Li, X., Li, R., 2017. Air pollution characteristics and their relation to meteorological conditions during 2014–2015 in major Chinese cities. Environ. Pollut. 223, 484–496. https://doi.org/10.1016/j.envpol.2017.01.050.

Huang, F., Li, X., Wang, C., Xu, Q., Wang, W., Luo, Y., Tao, L., Gao, Q., Guo, J., Chen, S., Cao, K., Liu, L., Gao, N., Liu, X., Yang, K., Yan, A., Guo, X., 2015. $PM_{2.5}$ spatiotemporal variations and the relationship with meteorological factors during 2013-2014 in Beijing, China. PloS One 10 (11), e0141642. https://doi.org/10.1371/journal.pone.0141642.

Kok, J.F., Ward, D.S., Mahowald, N.M., Evan, A.T., 2018. Global and regional importance of the direct dust-climate feedback. Nat. Commun. 9 (1), 241. https://doi.org/10.1038/s41467-017-02620-y.

Lai, S., Zhao, Y., Ding, A., Zhang, Y., Song, T., Zheng, J., Ho, K.F., Lee, S., Zhong, L., 2016. Characterization of PM $_{2.5}$, and the major chemical components during a 1-year campaign in rural Guangzhou, Southern China. Atmos. Res. 167, 208–215. https://doi.org/10.1016/j.atmosres.2015.08.007.

Li, X., Ma, Y., Wang, Y., Liu, N., Hong, Y., 2017. Temporal and spatial analyses of particulate matter (PM $_{10}$ and PM $_{2.5}$) and its relationship with meteorological parameters over an urban city in northeast China. Atmos. Res. 198, 185–193. https://doi.org/10.1016/j.atmosres.2017.08.023.

Li, Y., Yan, J., Sui, X., 2012. Tropospheric temperature inversion over central China. Atmos. Res. 116 (116), 105–115. https://doi.org/10.1016/j.atmosres.2012.03.009.

Lin, G., Fu, J., Jiang, D., Wang, J., Wang, Q., Dong, D., 2015. Spatial variation of the relationship between $PM_{2.5}$ concentrations and meteorological parameters in China. BioMed Res. Int. 2015 (21), 259–265. https://doi.org/10.1155/2015/684618.

Liu, Y., 2005. A study on zoning "New Three Macro-Regional Development Zones" of regional economy of China. Acta Geograph. Sin. 60 (3), 361–370. https://doi.org/10.11821/xb200503002.

Lu, D., Xu, J., Yang, D., Zhao, J., 2017. Spatio-temporal variation and influence factors of $PM_{2.5}$ concentrations in China from 1998 to 2014. Atmos. Pollut. Res. 8, 1151–1159. https://doi.org/10.1016/j.apr.2017.05.005.

Ma, Z., Hu, X., Sayer, A.M., Levy, R., Zhang, Q., Xue, Y., Tong, S., Bi, J., Huang, L., Liu, Y., 2016. Satellite-based spatiotemporal trends in $PM_{2.5}$ concentrations: China, 2004–2013. Environ. Health Perspect. 124 (2), 184–192. https://doi.org/10.1289/ehp.1409481.

Ocak, S., Turalioglu, F.S., 2008. Effect of meteorology on the atmospheric concentrations of traffic-related pollutants in Erzurum, Turkey. J. Int. Environ. Appl. Sci. 3 (5), 325–335.

Pitz, M., Schmid, O., Heinrich, J., Birmili, W., Maguhn, J., Zimmermann, R., Wichmann, H., Peters, A., Cyrys, J., 2008. Seasonal and diurnal variation of $PM_{2.5}$ apparent particle density in urban air in Augsburg, Germany. Environ. Sci. Technol. 42 (14), 5087–5093. https://doi.org/10.1021/es7028735.

Rebekić, A., Lončarić, Z., Petrović, S., Marić, S., 2015. Pearson's or spearman's correlation coefficient - Which one to use? Poljoprivreda 21 (2), 47–54. https://doi.org/10.18047/poljo.21.2.8.

Sandeep, A., Rao, T.N., Ramkiran, C.N., Rao, S.V.B., 2014. Differences in atmospheric boundary-layer characteristics between wet and dry episodes of the Indian summer monsoon. Bound-Lay. Meteorol. 153 (2), 217–236. https://doi.org/10.1007/s10546-014-9945-z.

Song, H., Wang, K., Zhang, Y., Hong, C., Zhou, S., 2017. Simulation and evaluation of dust emissions with WRF-Chem (v3.7.1) and its relationship to the changing climate over East Asia from 1980 to 2015, Atmos. Environ. Times 167, 511–522. https://doi.org/10.1016/j.atmosenv.2017.08.051.

Song, H., Zhang, K., Piao, S., Wan, S., 2016. Spatial and temporal variations of spring dust emissions in northern China over the last 30 years. Atmos. Environ. 126, 117–127. https://doi.org/10.1016/j.atmosenv.2015.11.052.

Tai, A.P.K., Mickley, L.J., Jacob, D.J., 2010. Correlations between fine particulate matter ($PM_{2.5}$) and meteorological variables in the United States: implications for the sensitivity of $PM_{2.5}$ to climate change. Atmos. Environ. 44 (32), 3976–3984. https://doi.org/10.1016/j.atmosenv.2010.06.060.

Tian, G., Qiao, Z., Xu, X., 2014. Characteristics of particulate matter (PM_{10}) and its relationship with meteorological factors during 2001-2012 in Beijing. Environ. Pollut. 192 (192), 266–274. https://doi.org/10.1016/j.envpol.2014.04.036.

Tie, X., Wu, D., Brasseur, G., 2009. Lung cancer mortality and exposure to atmospheric aerosol particles in Guangzhou, China. Atmos. Environ. Times 43 (14), 2375–2377. https://doi.org/10.1016/j.atmosenv.2009.01.036.

Trivedi, D.K., Ali, K., Beig, G., 2014. Impact of meteorological parameters on the development of fine and coarse particles over Delhi. Sci. Total Environ. 478 (1), 175. https://doi.org/10.1016/j.scitotenv.2014.01.101.

Wang, Y.Q., Zhang, X.Y., Sun, J.Y., Zhang, X.C., Che, H.Z., Li, Y., 2015. Spatial and temporal variations of the concentrations of PM_{10}, $PM_{2.5}$ and PM_1 in China. Atmos. Chem. Phys. 15 (23), 13585–13598. https://doi.org/10.5194/acp-15-13585-2015.

Wang, Y., Ying, Q., Hu, J., Zhang, H., 2014. Spatial and temporal variations of six criteria air pollutants in 31 provincial capital cities in China during 2013–2014.

Environ. Int. 73, 413–422. https://doi.org/10.1016/j.envint.2014.08.016.
Whiteman, C.D., Hoch, S.W., Horel, J.D., Charland, A., 2014. Relationship between particulate air pollution and meteorological variables in Utah's Salt Lake Valley. Atmos. Environ. 94, 742–753. https://doi.org/10.1016/j.atmosenv.2014.06.012.
Wu, P., Ding, Y., Liu, Y., 2017. Atmospheric circulation and dynamic mechanism for persistent haze events in the Beijing-Tianjin-Hebei region. Adv. Atmos. Sci. 34 (4), 429–440. https://doi.org/10.1007/s00376-016-6158-z.
Xie, Y., Zhao, B., Zhang, L., Luo, R., 2015. Spatiotemporal variations of $PM_{2.5}$ and PM_{10} concentrations between 31 Chinese cities and their relationships with SO_2, NO_2, CO and O_3. Particuology 20, 141–149. https://doi.org/10.1016/j.partic.2015.01.003.
Xu, J., Yan, F., Xie, Y., Wang, F., Wu, J., Fu, Q., 2015. Impact of meteorological conditions on a nine-day particulate matter pollution event observed in December 2013, Shanghai, China. Particuology 20 (3), 69–79. https://doi.org/10.1016/j.partic.2014.09.001.
Yang, B., Brauning, A., Zhang, Z., Dong, Z., Esper, J., 2007. Dust storm frequency and its relation to climate changes in Northern China during the past 1000 years. Atmos. Environ. 41 (40), 9288–9299. https://doi.org/10.1016/j.atmosenv.2007.09.025.
Yang, Q., Yuan, Q., Li, T., Shen, H., Zhang, L., 2017a. The relationships between $PM_{2.5}$ and meteorological factors in China: seasonal and regional variations. Int. J. Environ. Res. Publ. Health 14 (12), 1510. https://doi.org/10.3390/ijerph14121510.
Yang, Y., Liu, X., Qu, Y., Wang, J., An, J., Zhang, Y., Zhang, F., 2015. Formation mechanism of continuous extreme haze episodes in the megacity Beijing, China, in January 2013. Atmos. Res. 155, 192–203. https://doi.org/10.1016/j.atmosres.2014.11.023.
Yang, Y., Russell, L.M., Lou, S., Liao, H., Guo, J., Liu, Y., Singh, B., Ghan, S.J., 2017b. Dust-wind interactions can intensify aerosol pollution over Eastern China. Nat. Commun. 8, 15333. https://doi.org/10.1038/ncomms15333.
Yasunori, K., Masao, M., 2005. Regional difference in the characteristic of dust event in East Asia: relationship among dust outbreak, surface wind, and land surface condition. Journal. Meteorol. Soc. Jpn. 83A (3), 1–18. https://doi.org/10.2151/jmsj.83A.1.
Ye, W.F., Ma, Z.Y., Ha, X.Z., 2018. Spatial-temporal patterns of $PM_{2.5}$ concentrations for 338 Chinese cities. Sci. Total Environ. 631–632, 524–533. https://doi.org/10.1016/j.scitotenv.2018.03.057.
Yi, X.Y., Peng, Y.H., Liao, J.Y., Liu, Y., Li, G.F., 2017. A review of the relationship between forest vegetation and atmospheric particulate matter. Plant Sci. J (in Chinese). https://doi.org/10.11913/PSJ.2095-0837.2017.50790.
Zhang, H., Wang, Y., Hu, J., Ying, Q., Hu, X., 2015a. Relationships between meteorological parameters and criteria air pollutants in three megacities in China. Environ. Res. 140, 242–254 (A). https://doi.org/10.1016/j.envres.2015.04.004.
Zhang, B., Jiao, L.M., Xu, G., Zhao, S.L., Tang, X., Zhou, Y., Gong, C., 2018. Influences of wind and precipitation on different-sized particulate matter concentrations ($PM_{2.5}$, PM_{10}, $PM_{10-2.5}$). Meteorol. Atmos. Phys. 130 (3), 383–392. https://doi.org/10.1007/s00703-017-0526-9.
Zhang, Q., Quan, J., Tie, X., Li, X., Liu, Q., Gao, Y., Zhao, D., 2015b. Effects of meteorology and secondary particle formation on visibility during heavy haze events in Beijing, China. Sci. Total Environ. 502, 578–584. https://doi.org/10.1016/j.scitotenv.2014.09.079.
Zhang, Y.L., Cao, F., 2015. Fine particulate matter ($PM_{2.5}$) in China at a city level. Sci. Rep. 5, 14884. https://doi.org/10.1038/srep14884.
Zhao, S.P., Yu, Y., Yin, D.Y., He, J.J., Liu, N., Qu, J.J., Xiao, J.H., 2016. Annual and diurnal variations of gaseous and particulate pollutants in 31 provincial capital cities based on in situ air quality monitoring data from China National Environmental Monitoring Center. Environ. Int. 86, 92–106. https://doi.org/10.1016/j.envint.2015.11.003.
Zhu, J., Che, H., Xia, X., Chen, H., Goloub, P., Zhang, W., 2014. Column-integrated aerosol optical and physical properties at a regional background atmosphere in North China Plain. Atmos. Environ. 84 (2), 54–64. https://doi.org/10.1016/j.atmosenv.2013.11.019.